J. of Nuclear Sci. and Tech.
No. 52, pp. 80-86, 2009

مجله علوم و فنون هسته‌ای
شماره ۵۲، صفحات ۸۶-۸۰، ۱۳۸۹

Nuclear Radiations Induced Change in Thermal and Structural Properties of 2-{[4-(2-HydroxyBenzylideneamino) Phenylimino] Methyl} Phenol (PAM) Schiff Base

H.G. Mohammadi[1], R. Khodabakhsh[2,3], A. Hassanzadeh[*3]

1- Department of Physics, Faculty of Science, Urmia University, P.O. Box: , Urmia- Iran
2- Department of Chemistry, Faculty of Science, Urmia University, P.O. Box: , Urmia- Iran
3- Research Center of Nanotechnology of Urmia University, P.O. Box: , Urmia- Iran

Abstract: The variation of thermal and structural properties of 2-{[4-(2-hydroxybenzylideneamino) phenylimino]methyl}phenol (PAM) Schiff base were studied using differential scanning calorimetry (DSC) and powder X-ray diffraction techniques before and after fast neutron (1.050 and 1.740kGy), beta (11.01Gy) and gamma (453.0Gy) irradiations. Under fast neutron irradiation, the melting and decomposition enthalpies and temperatures were changed with increasing the irradiation time. The kinetic parameters were calculated using both model free isoconversional and Kissinger analysis methods. Gamma irradiation showed similar effect on structural and thermal properties.

Keywords: ***Schiff Base, Model- Free Isoconversional Method, Kissinger Analysis Method, Fast Neutron, Beta, Gamma Irradiations.***

1- Introduction

Schiff bases have been widely used as protective group of amino group in organic synthesis [1-4]. A Schiff base can be hydrolyzed with water to the corresponding amine and carbonyl compounds and was carefully investigated by Jencks [5,6]. The hydrolysis of Schiff bases in the presence of water and acetone under UV (sun) light has also been reported [7]. Schiff bases have received a considerable amount of attention from many researchers owing to their importance in exhibiting thermochromism and photochromism [8]. Metal complexes of Schiff bases are extensively studied due to synthetic flexibility, selectivity and sensitivity towards a variety of metal atoms [9]. They are found useful in catalysis, in medicine as antibiotics and anti-inflammatory agents and in the industry as anticorrosion [10-16].

Ionizing radiations, including alpha and beta particles, gamma rays, X-rays, neutrons and protons have serious effects on Schiff base compounds. The aim of this paper is to investigate the effects of fast neutron, beta and gamma radiations on novel synthesized radioactive rays influences on 2-{[4-(2-hydroxybenzylideneamino) phenylimino] methyl} phenol (PAM) Schiff base as a case study.

2- Experimental

2-1 Materials and Instrument

2-{[4-(2-hydroxybenzylideneamino) phenylimino] methyl} phenol (PAM) Schiff base was prepared according to the following route, using para aminoaniline and salicyl aldehyde in EtOH under 6h reflux. PAM is a crystalline material with molecular formula $C_{20}H_{16}N_2O_2$, and molecular weight 316.12g/mol. Scheme 1 shows its chemical structure and the synthesis path of the molecule.

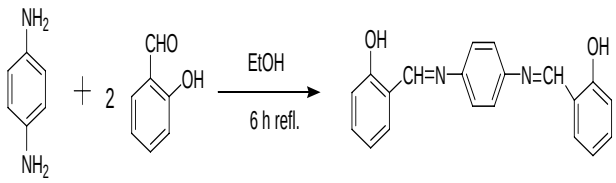

Scheme 1. Synthesis path and chemical structure of Schiff base of 2-{[4-(2-hydroxybenzylideneamino) phenylimino]methyl}phenol (PAM).

*email: ali.hassanzadeh@gmail.com

Date of Receipt: 1388/12/22 Date of Admission: 1389/3/15

2-2 Irradiation procedure

Samples were irradiated with fast neutrons produced from a $^{241}Am–^{10}Be$ (Radiochemical, Amersham, UK) neutron source with a flux density of 2.82×10^{8} cm^{-2} s^{-1} and with the dose rate of 4.07 Gy/h; and with the gamma ray produced from a ^{137}Cs gamma source (20 mCi) with a flux density of 7.50×10^{6} cm^{-2} s^{-1} and with the dose rate of 6.12 Gy/h. Beta ray was produced from a ^{90}Sr source (3 micro Ci) with a flux density of 0.44×10^{4} cm^{-2} s^{-1} and with the dose rate of 0.15 Gy/h.

2-3 Apparatus

Thermal analysis was performed using DSC823^{e} Mettler Toledo Stare system instrument. The heating rate was $10Kmin^{-1}$, unless stated elsewhere. XRD measurements were performed using X'Pert Philips X-ray diffractometer at room temperature with monochromated CuK_{α} (l =1.54 Å) in the scan range of 2θ between 15° and 70° with a step size of 0.02 (2θ/s).

3- Results and discussion

3-1 Fast neutron irradiation effect on thermal behavior

Fig. 1 shows the differential scanning calorimetry (DSC) trace of PAM; before (top), and after 1.05 kGy (middle), 1.74 kGy (down) fast neutron irradiation with the heating rate of 10 K min^{-1}. As it is seen, PAM exhibits two endothermic peaks and one exothermic peak before the irradiation. Berzelius first used the term allotropy when an element was found to exist in two or more forms possessing different properties. Later, Ostwald included compounds as well, and defined allotropism as the phenomenon in which a substance, element or compound could exist in two or more forms, exhibiting different properties, either physical or chemical. In the case of solid allotropes, the term polymorphism is more commonly used. A solid which occurs in two forms is said to be dimorphous, in three trimorphous, etc, [17]. It seems that PAM has many forms, therefore it is a polymorphous compound. Hence, the first weak peak at 192.58°C relates to melting of one form of PAM. The second sharp peak at 215.44°C relates to melting of other form of PAM. The third sharp exothermic peaks at 363.74°C relates to decomposition of two forms of PAM. The position and enthalpy values of these endothermic and exothermic peaks before and after the fast neutron irradiation are listed in Table 1. It is clear that the endothermic peaks of enthalpy values and positions decrease by increasing the irradiation time. It means that the melting of PAM readily occurs under the irradiation. This behavior can be rationalized on the base of the fact that the effect of irradiation on chemical compounds is believed to depend on the type and energy of irradiation, its composition and sample parameters. It is well established that the radiation damage in crystalline compounds leads to active defects. These defects can be introduced by ionization or atomic displacement mechanisms or via the activation of the preexisting defects. These defects may be either permanent or temporary. The presence of defects and irradiation-induced disorders affects significantly the characteristic features of DSC thermogram, such as melting and decomposition temperatures and their enthalpy values.

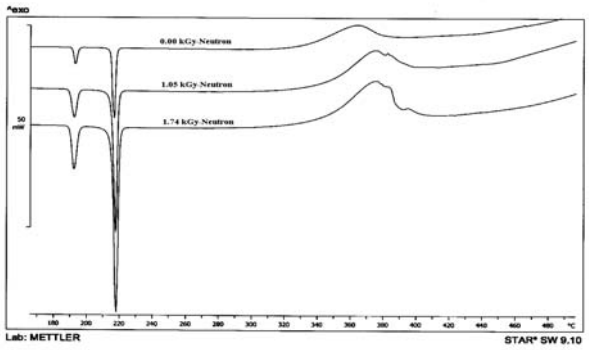

Fig. 1. DSC thermograms of PAM before (top), after 1.05kGy (middle) and 1.74kGy (down) fast neutron irradiation with heating rate of 10 $Kmin^{-1}$.

Table 1. Position and enthalpy values of endothermic peaks of PAM before and after fast neutron irradiation and exothermic.

	Peak 1 (°C)	(J/g)	Peak 2 (°C)	(J/g)	Peak 3 (°C)	(J/g)
Before irradiation	192.58	+36.73	215.44	+148.37	363.74	-464.96
After 1.05 kGy irradiation	191.69	+24.61	215.29	+99.55	374.79	-163.05
After 1.74 kGy irradiation	191.25	+27.40	214.92	+110.24	375.16	-218.71

Fig. 2 shows the DSC thermograms of PAM at heating rates of 10, 20, 30, 60, 70 and 80 $Kmin^{-1}$ before fast neutron irradiation. Similar thermograms were obtained for other irradiation times (not shown here). The melting and boiling transitions are kinetically determined (time-dependent) transitions, and thus the temperature at which they are detected depends on the heating rate used to measure them. As shown, the position of the first and second endothermic peaks depends fairly on the heating rate. But in comparison with the other peaks the shape and position of the third exothermic peak depends strongly on the heating rate.

Fig. 3 shows the DSC thermogram of PAM at heating rates of 10, 20, 30, 50, 60, 70 and 80$Kmin^{-1}$ after 1.74kGy fast neutron irradiation. It is clear that the characteristic features of thermograms are changed upon irradiation. It has been suggested that the interaction of fast neutrons with a chemical compound results in the rupture of chemical bonds, the displacement of electrons and ions, and the creation of highly energetic alpha particles. Displaced electrons, ions and recoils, migrate through the solid network until they are trapped by either the matrix defects or the presence of a transition metal element in the lattice, leaving deficient regions.

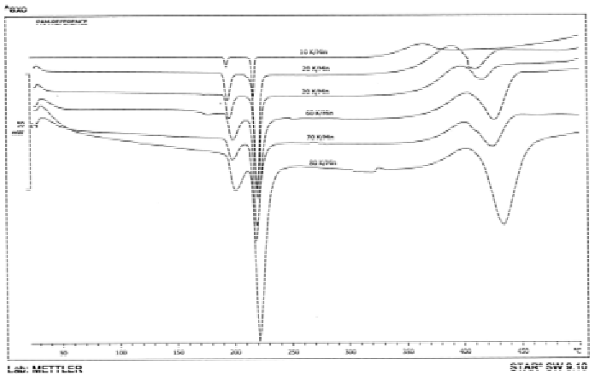

Fig. 2. DSC thermograms of PAM before fast neutron irradiation at different heating rates.

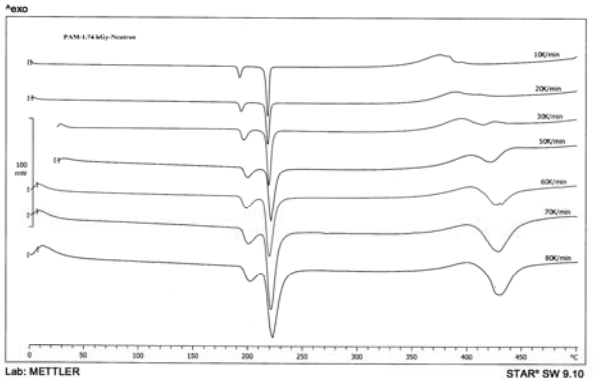

Fig. 3. DSC thermograms of PAM at different heating rates after 1.74kGy fast neutron irradiation.

3-2 Kinetic theory

The theory of this research is based on the equation of kinetics:

$$\frac{d\alpha}{dt} = f(\alpha) \times k(T) \qquad (1)$$

$$k(T) = k_0 \times \exp(\frac{-E_a}{RT}) \qquad (2)$$

where E_a is the activation energy of reaction, k_0 is the pre-factor, R is the gas constant, and α is the degree of conversion. $f(\alpha)$ is the reaction model for a certain reaction. The data of DSC scans have been used to calculate the activation energy and pre-factor employing the following methods:

(i)Method of Kissinger-Akahira-Sunose (KAS)

This method develops from the assumption that, during the rise in temperature, the reaction passes by a maximum before decreasing; it is based on the following relation:

$$\ln(\frac{T_P^2}{\beta}) = \ln(\frac{E_a}{R \times k_0}) + (\frac{E_a}{R}) \times \frac{1}{T_P} \qquad (3)$$

Eq. (3) shows that a linear relation exists between $\ln(T_p^2/\beta)$ versus $1/T_p$, with (E_a/R) as the slope and the value of pre-exponential factor of rate constant in terms of natural logarithm. Thus, one can determine both parameters using KAS method.

Figs. 4 and 5 show the plot of $\ln(T^2/\beta)$ versus 1000/T for PAM before and after 1.74kGy fast neutron irradiation. Unlike the isoconversional methods, the KAS method takes a simplified approach that yields only a single E_a value for the whole process. The activation energy can be calculated from the

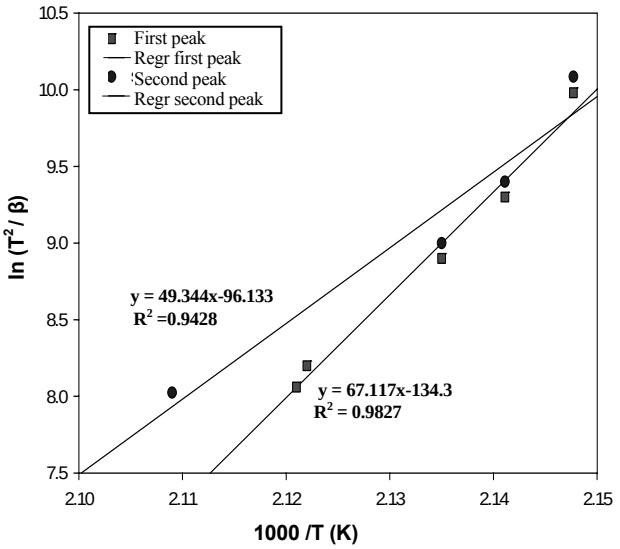

Fig. 4. Plot of ln (T^2/β) versus 1000/T plot of PAM (the first and second endothermic peaks) before fast neutron irradiation.

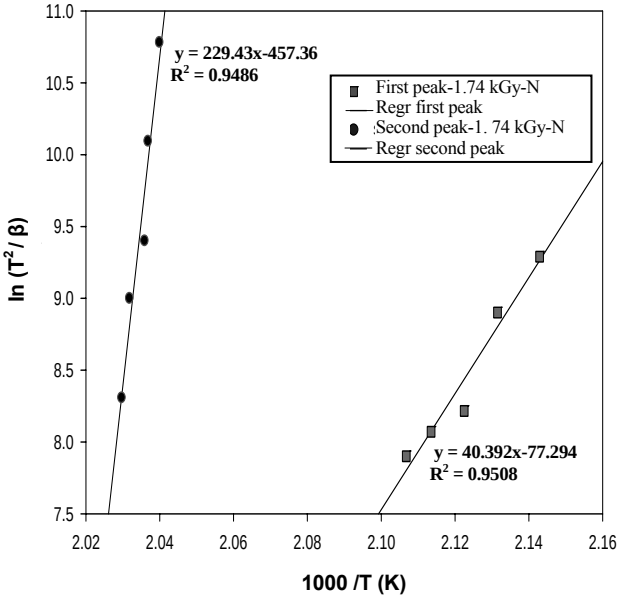

Fig. 5. Plot of ln(T^2/β) versus 1000/T of PAM (the first and second endothermic peaks) after 1.74kGy fast neutron irradiation.

linear portions of plots. The calculated E_a from the variation of the first and second endothermic peaks of PAM before irradiation are 558.01 and 410.24kJ/mol, respectively. Also, the calculated E_a after 1.74kGy fast neutron irradiation for the first and second peaks are 335.82 and 1867.56kJ/mol, respectively. It is clear that the fast neutron irradiation has reduced the activation energy of reaction.

(ii) Model free isoconversional method analysis.

Simple models such as KAS provide very little specific information on the various thermal events happening during the reactions such as variation of E_a with the degree of conversion (α). They also fail to establish whether the process undergoes a single or multi-step kinetics. In this context, isoconversional methods provide more details as they determine the E_a dependence with respect to α. The heat flow values recorded from the non-isothermal DSC experiments can be converted to α.

$$\alpha = \frac{S_T}{S} \tag{4}$$

where S_T is the sample peak area from 0 to T, S is the total sample peak area, and β is the heating rate. An isoconversional method in which DSC scans are taken at a series of heating rates can be used to obtain kinetic parameters, and the apparent activation can be obtained from the following equation [18].

$$\ln(\beta) = C - (\frac{E_\alpha}{R}) \times \frac{1}{T_\alpha} \tag{5}$$

C is a constant, β is the heating rate, E_α and T_α are the apparent activation energy and temperature at a specific degree of conversion α. The advantage of this isoconversional method is that the activation energy can be obtained without specifying a certain reaction model, therefore, this method is a model-free one [18].

The first endothermic peak areas in Fig. 2 were used to obtain the plots of α versus T. Fig. 6 shows the variation of α with temperature (T) during the first melting peak of PAM at various heating rates. Figs. 7 and 8 show the plot of ln(β) versus 1000/T for PAM before and after 1.74kGy fast neutron irradiation, respectively. Eq. (5) shows that a linear relation exists between ln(β) versus $1/T_\alpha$, with (E_α/R) as the slope and the value of pre-exponential factor of the rate constant in terms of natural logarithm. Thus, one can determine both parameters using model- free method.

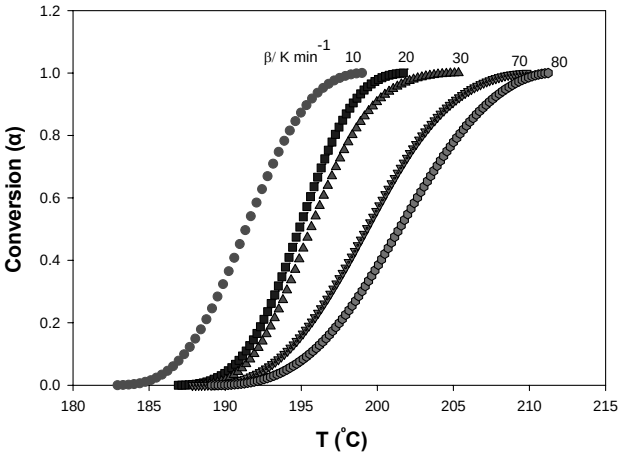

Fig. 6. Degree of conversion (α) as a function of temperature (T) at different heating rate for the first peak of PAM before fast neutron irradiation.

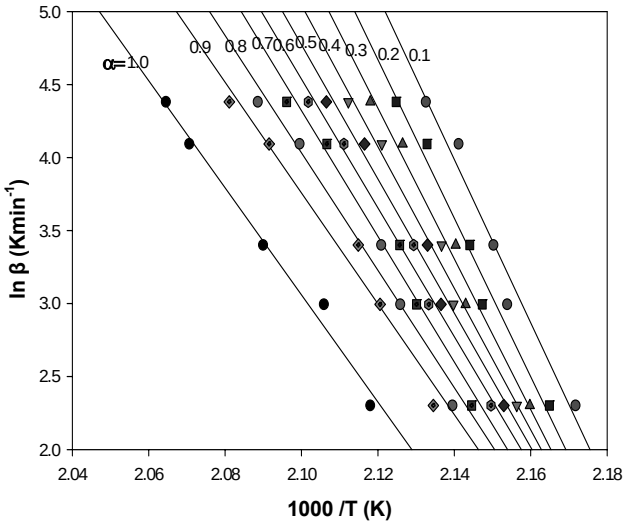

Fig. 7. Plot of ln(β) versus 1000/T of PAM (the first peak) before fast neutron irradiation.

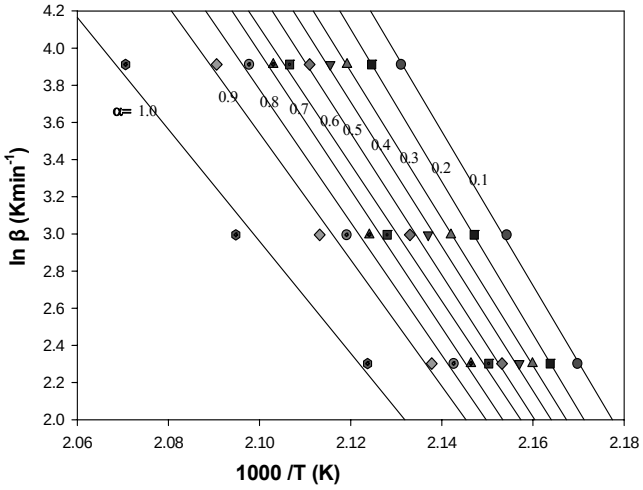

Fig. 8. Plot of ln(β) versus 1000/T of PAM (the first peak) after 1.74 kGy fast neutron irradiation.

Fig. 9 shows the dependence of E_α of PAM (the first peak) after 1.74kGy fast neutron irradiation on conversion degree (α). As can be seen, a great dependence of E_a on α was observed for irradiated sample, indicating a complex process.

3-3 Fast neutron irradiation effect on structural properties

The powder X-ray diffraction (XRD) patterns of PAM, before (or reference) and after 1.74kGy fast neutron, 11.1Gy beta and 453Gy gamma irradiation are shown in Fig. 10. As can be seen, their profile positions do not significantly differ but the intensity of certain orientations after fast neutron and gamma irradiation increase.

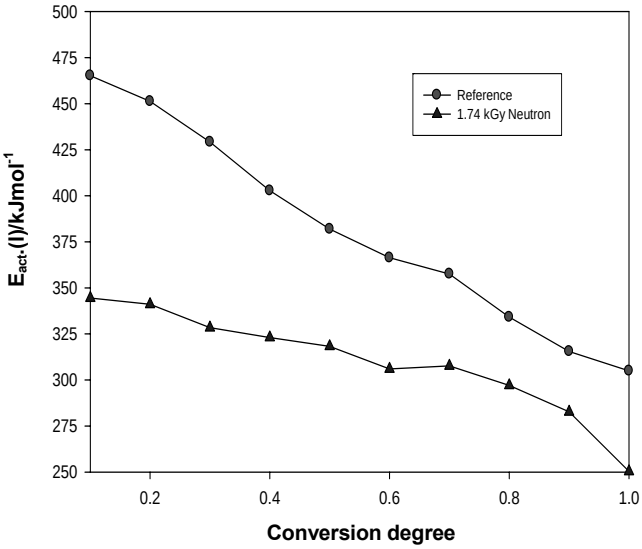

Fig. 9. The dependence of E_α of PAM (the first peak) on conversion (α) after 1.74kGy fast neutron irradiation.

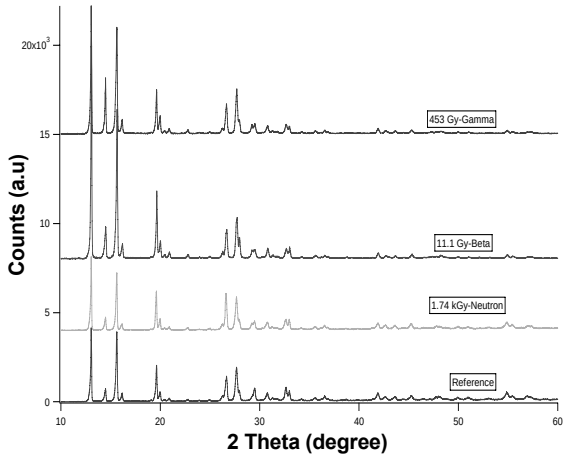

Fig. 10. XRD patterns of PAM: before (or reference) and after 1.74kGy fast neutron, 11.1Gy beta and 453Gy gamma irradiation.

3-4 Beta and gamma irradiations effect on thermal behavior

Fig. 11 shows the DSC thermograms of PAM before and after 1.05kGy, 1.74kGy fast neutron, 11.1Gy beta and 453Gy gamma irradiations with the heating rate of 10 $Kmin^{-1}$. By comparison, it is evident that the lower absorbed doses of gamma have produced a significant effect on thermal properties. Gamma irradiation of chemical compounds is reported to lead mainly to surface damage, unstable charging, and migration of mobile (non-network) cations [19].

4. Conclusion

The results showed that the irradiation of PAM with either fast neutrons or beta and gamma ones clearly affects the structural and thermal properties. The thermal analysis result suggests that PAM is a polymorphous compound. Model- free isoconversional analysis suggests a great dependence of E_a on α observed for irradiated sample, which indicates a complex process. Our findings show that the thermal analysis is more sensitive than the XRD technique for studying the nuclear radiations induced changes on PAM.

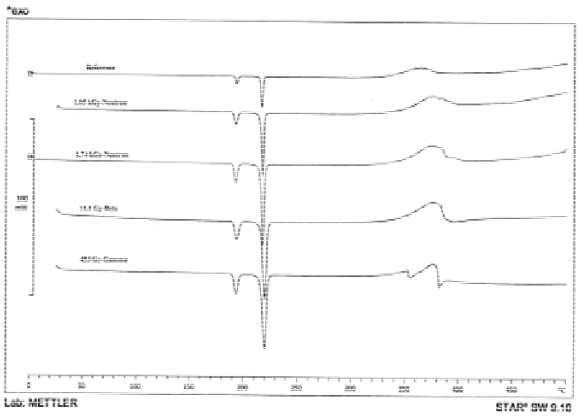

Fig. 11. DSC thermograms of PAM before and after 1.05, 1.74kGy fast neutron, 11.1 Gy beta and 453 Gy gamma irradiations with heating rate of 10 $Kmin^{-1}$.

References:

1. P. Bey, J. P.Vevert, Preparation of Schiff bases of aminocycloalkanecarboxylic acids esters, Tetrahedron Lett. 18 (1977)1455-1458.

2. R. A. Lucas, D. F. Dickel, M. J. Dziemian, B. L. Hensle, and H. B. MacPhillamy, 3,4-Dimethoxy-N-(4-nitrobenzylidene)aniline , J. Am. Chem. Soc. 82(1960) 5688- 5693.

3. G. W. J. Fleet and I. Fleming, Hydrolysis of Schiff Bases Promoted by UV Light, J. Chem. Soc. C (1969)1758 -1763.

4. B. Bezas and L. Zervas, Crystal structure of N-(diphenylmethylene) diphenylmethanamine, C26H21N,J. Am. Chem. Soc. 83 (1961) 719 – 722.

5. W. P. Jencks, Effect of the nonreducing end of Shigella dysenteriae type 1 O-specific oligosaccharides on their immunogenicity as conjugates in mice, J. Am. Chem. Soc. 81 (1959) 475−481.

6. B. M. Anderson, W. P. Jencks, The Effect of Structure on Reactivity in Semicarbazone Formation, J. Am. Chem. Soc. 82 (1960) 1773-1777.

7. Z. Huang, D. Wan, J. Huang, Hydrolysis of Schiff Bases Promoted by UV Light, Chemistry Letters, 5 (2001) 708-716.

8. E. Hadjoudis, M. Vittorakis, I. Moustakali-Mavridis, Photochromism and thermochromism of schiff bases in the solid state and in rigid glasses,Tetrahedron 43 (1987)1345-1360.

9. C. Spinu, A. Kriza, Co(II), Ni(II) and Cu(II) COMPLEXES OF BIDENTATE SCHIFF BASES,Acta Chim. Slov. 47 (2000) 179-185.

10. B. Sun, J. Chen, J. Y. Hu, X. Li, Dioxygen affinity and catalytic performance of bis-(furaldehyde) Schiff bases Co(II) complexes in cyclohexene oxidation, J. Chin. Chem. Lett. 12 (2001)1043-1046.

11. D. M. Boghaei, S. Mohebi, Synthesis, characterization and study of vanadyl tetradentate Schiff base complexes as catalyst in aerobic selective oxidation of olefins, Tetrahedron 58 (2002) 5357-5366.

12. J. Liu, B. Wu, B. Zhang, Y. Liu, Synthesis and Characterization of Metal Complexes of Cu(II), Ni(II), Zn(II), Co(II), Mn(II) and Cd(II) with Tetradentate Schiff Bases, Turk. J. Chem. 30 (2006) 41-48.

13. G. J. P. Britovsek, V. V. Gibson, S. Mastroianni, D. C. H. Oakes, C. Redshaw, G. A. Solan, A. J. P. White, D. J. Williams, Imine Versus Amine Donors in Iron-Based Ethylene Polymerisation Catalysts, Eur. J. Inorg. Chem. 2001 (2001) 431-437.

14. A. Budakoti, M. Abid, A. Azam, Synthesis and antiamoebic activity of new 1-N-substituted thiocarbamoyl-3,5-diphenyl-2-pyrazoline derivatives and their Pd(II) complexes, Eur. J. Med. Chem. 41 (2006) 63-70.

15. V. X. Jin, S. I. Tan, J. D. Ranford, Platinum(II) triammine antitumour complexes: structure-activity relationship with guanosine 5'-monophosphate (5'-GMP), Inorg. Chim. Acta 358 (3) (2005) 677-686.

16. A. A. Osowole, Syntheses and characterization of some tetradentate Schiff-Base complexes and their heteroleptic analogues, E-Journal of Chemistry, 5 (2008) 130-135.

17. P. C. Rakshit, Physical Chemistry, 1st Edition, Sadhana Press Private Limited, London, 1969, pp. 200-201.

18. Vyazovkin S., Modification of the integral isoconversional method to account for variation in the activation energy, J. Comput. Chem. 22, (2001)178–183.

19. Ezz-Eldin F. M., El-Alaily N. A., El-Batal H.A., Density and refractive index of some γ-irradiated alkali silicate glasses, Ind. J. Pure Appl. Phys. 30 (1992) 443-448.